Amyloid-β overproduction causes abnormal mitochondrial dynamics via differential modulation of mitochondrial fission/fusion proteins

Xinglong Wang[a], Bo Su[a], Sandra L. Siedlak[a], Paula I. Moreira[b], Hisashi Fujioka[c], Yang Wang[d], Gemma Casadesus[e], and Xiongwei Zhu[a,1]

Departments of [a]Pathology, [c]Pharmacology, [d]Biostatistics and Epidemiology, and [e]Neuroscience, Case Western Reserve University, Cleveland, OH 44106; and [b]Center for Neuroscience and Cell Biology, University of Coimbra, 3005-504 Coimbra, Portugal

Edited by Lennart Mucke, Gladstone Institute of Neurological Disease, San Francisco, CA, and accepted by the Editorial Board October 3, 2008 (received for review May 21, 2008)

Mitochondrial dysfunction is a prominent feature of Alzheimer disease but the underlying mechanism is unclear. In this study, we investigated the effect of amyloid precursor protein (APP) and amyloid β on mitochondrial dynamics in neurons. Confocal and electron microscopic analysis demonstrated that ≈40% M17 cells overexpressing WT APP (APPwt M17 cells) and more than 80% M17 cells overexpressing APPswe mutant (APPswe M17 cells) displayed alterations in mitochondrial morphology and distribution. Specifically, mitochondria exhibited a fragmented structure and an abnormal distribution accumulating around the perinuclear area. These mitochondrial changes were abolished by treatment with β-site APP-cleaving enzyme inhibitor IV. From a functional perspective, APP overexpression affected mitochondria at multiple levels, including elevating reactive oxygen species levels, decreasing mitochondrial membrane potential, and reducing ATP production, and also caused neuronal dysfunction such as differentiation deficiency upon retinoic acid treatment. At the molecular level, levels of dynamin-like protein 1 and OPA1 were significantly decreased whereas levels of Fis1 were significantly increased in APPwt and APPswe M17 cells. Notably, overexpression of dynamin-like protein 1 in these cells rescued the abnormal mitochondrial distribution and differentiation deficiency, but failed to rescue mitochondrial fragmentation and functional parameters, whereas overexpression of OPA1 rescued mitochondrial fragmentation and functional parameters, but failed to restore normal mitochondrial distribution. Overexpression of APP or Aβ-derived diffusible ligand treatment also led to mitochondrial fragmentation and reduced mitochondrial coverage in neuronal processes in differentiated primary hippocampal neurons. Based on these data, we concluded that APP, through amyloid β production, causes an imbalance of mitochondrial fission/fusion that results in mitochondrial fragmentation and abnormal distribution, which contributes to mitochondrial and neuronal dysfunction.

amyloid precursor protein | DLP1 | mitochondrial fragmentation | OPA1 | perinuclear accumulation

Alzheimer disease (AD) is the most common neurodegenerative disorder in the aged population and is characterized by extensive regionalized neuronal loss and the presence of neurofibrillary tangles and senile plaques in the brain. Senile plaques are deposits of amyloid-β (Aβ), a 39–43-aa peptide produced by the sequential cleavage of β- and γ-secretase at the C terminus of amyloid precursor protein (APP) (1). More than 20 mutations in APP have been linked to familial AD (fAD) that have altered APP processing with respect to enhanced Aβ generation or aggregation (2). Despite intensive focus on APP and Aβ, the exact mechanisms responsible for the massive neurodegeneration in early-stage fAD are incompletely resolved.

Persuasive evidence suggests that oxidative stress is one of the earliest changes and plays an important role in the pathological process in AD (3). Increased oxidative stress levels have been found in the brains of patients with fAD in Sweden and early in Tg2576 APP transgenic mice (4, 5), suggesting that fAD-associated mutations probably enhance oxidative stress. Mitochondria are the major source of reactive oxygen species (ROS) and, in fact, mitochondrial dysfunction, as well as hypometabolism, have long been implicated in the onset of the familial and sporadic forms of AD (6). mtDNA defects have also been linked to an increased incidence of AD (7, 8). Quantitative morphometric analysis of mitochondria shows increased abnormal and damaged mitochondria in AD (9, 10). Multiple lines of evidence support APP and Aβ as contributing factors to mitochondrial dysfunction in AD: both APP and Aβ are present in mitochondrial membrane and interact with mitochondrial proteins, block mitochondrial import channels, impair mitochondrial transport, disrupt the electron transfer chain, increase ROS levels, and cause mitochondrial damage (11–15).

A number of recent studies demonstrated that mitochondria are dynamic organelles undergoing continual fission and fusion (16). In mammalian cells, fission requires Fis1 and dynamin-like protein (DLP1). Conversely, fusion involves OPA1, Mfn1, and Mfn2 (17). Unbalanced fusion leads to mitochondrial elongation and unbalanced fission leads to excessive mitochondrial fragmentation, both of which impair mitochondrial function (18, 19). Impairments in mitochondrial dynamics are being increasingly implicated in neurodegenerative diseases (16). Very recently, we reported abnormal mitochondrial fission and fusion in AD fibroblasts (20). In this study, we aimed to determine whether APP and Aβ cause mitochondrial dysfunction and neuronal dysfunction through modulation of mitochondrial dynamics.

Results

Generation of Stable M17 Cell Lines Overexpressing APP. To investigate the effects of APP overexpression on mitochondrial dynamics in neuronal cells, three independent clones of M17 cells stably transfected with WT APP cDNA (APPwt M17 cells) or APP Swedish mutant cDNA (APPswe M17 cells) were established. Overexpression of APP in these lines was confirmed by Western blotting (Fig. 1*A*). There was no increase in basal cell death in any of these cell lines compared with control cells (i.e., untransfected or empty vector-transfected cells; not shown). No cell processes, or only very short ones, were seen in control or transfected cells before differentiation. Interestingly, upon RA treatment at 1 month, the majority (>75%) of control cells extended long and branched neurites, but only 19.4% ± 4.9% APPwt cells and no APPswe M17

Author contributions: X.Z. designed research; X.W., B.S., S.L.S., and H.F. performed research; X.W., P.I.M., H.F., Y.W., G.C., and X.Z. analyzed data; and X.W. and X.Z. wrote the paper.

The authors declare no conflict of interest.

This article is a PNAS Direct Submission. L.M. is a guest editor invited by the Editorial Board.

[1]To whom correspondence should be addressed. E-mail: xiongwei.zhu@case.edu.

This article contains supporting information online at www.pnas.org/cgi/content/full/0804871105/DCSupplemental.

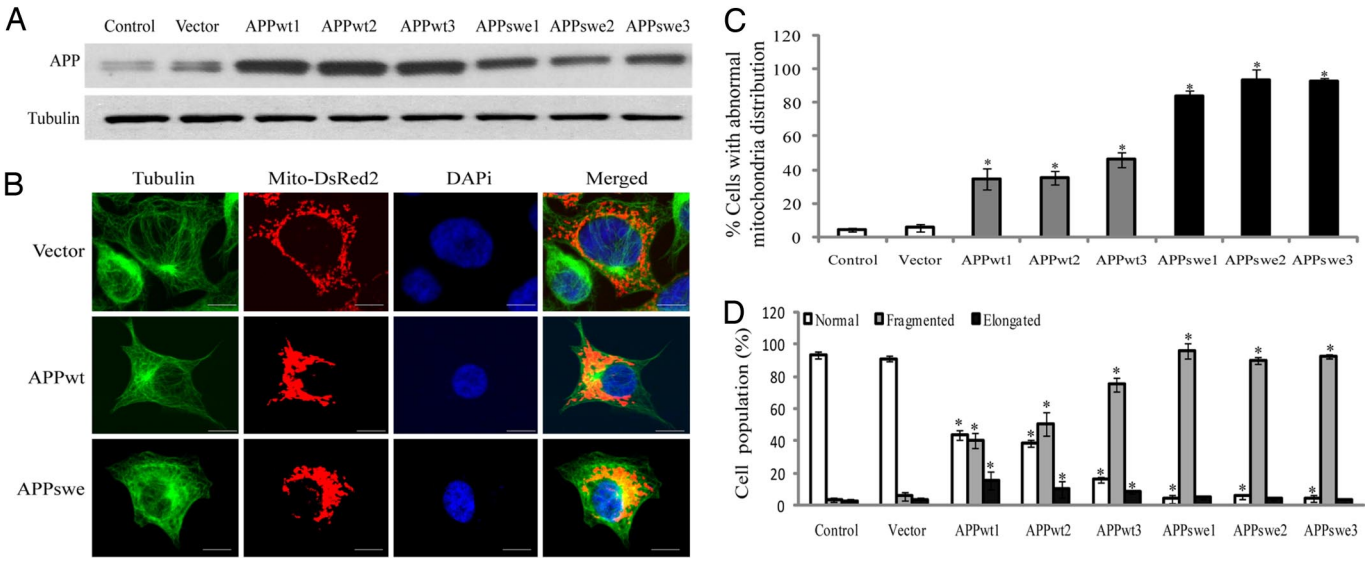

Fig. 1. APP causes abnormal mitochondrial dynamics in M17 cells. (*A*) Representative immunoblot of APP. Tubulin is used as an internal loading control. (*B*) Representative pictures of stable M17 lines with different mitochondrial distribution patterns are shown. Green, tubulin; red, mito-DsRed2; blue, DAPi. Mitochondrial distribution (*C*) and morphology (*D*) are analyzed. At least 1,000 cells were measured for each cell line. (Scale bars, 10 μm.) *, $P < 0.05$, Student *t* test.

cells extended neurites, suggestive of no differentiation. Therefore, we used M17 cells in undifferentiated status in all of the following studies.

Effects of APP Expression on Mitochondrial Dynamics. To visualize mitochondria, stable M17 cell lines were transiently transfected with Mito-DsRed 2. Forty-eight hours after transfection, cells were fixed, stained, and evaluated using laser confocal microscopy (Fig. 1*B*). Mitochondrial distribution was strikingly different in APPwt and APPswe M17 cells compared with control cells (i.e., untransfected or empty vector-transfected cells): in control cells, mitochondria were distributed evenly throughout the cytoplasm (>95% cells; Fig. 1 *B* and *C*). However, in APPwt M17 cells, 30% to 50% cells demonstrated an abnormal distribution with mitochondria accumulating around the perinuclear area whereas more remote cytoplasmic areas were devoid of mitochondria (Fig. 1 *B* and *C*). It became more severe in APPswe M17 cells, in which 80%–95% cells exhibited such abnormal mitochondrial distribution (Fig. 1 *B* and *C*).

As to mitochondrial morphology, most control cells (>95%) exhibited normal short tubular mitochondria (Fig. S1*B*). Conversely, in APPwt M17 cells, whereas 20%–40% cells displayed such normal short tubular mitochondria as control cells (Fig. 1*D*), 40%–60% of the APPwt M17 cells had a fragmented, punctiform structure of mitochondria (Fig. S1*B*), and a small population (10%–15%) showed an elongated, net-like structure of mitochondria (Fig. S1*B*). It again became more severe in APPswe M17 cells, in which the percentage of cells with fragmented mitochondria exceeded 80% (Fig. 1*D*).

Consistent with our confocal microscopic studies, electron microscopic studies on mitochondria in these stable lines showed a similar pattern of mitochondrial alterations such that the majority of empty vector-transfected control cells exhibited even mitochondrial distribution (Fig. S2*A*) whereas APPwt (Fig. S2*B*) and APPswe M17 cells (Fig. S2*C*) exhibited abnormal mitochondria accumulation around the perinuclear area. Long and thin mitochondria were abundant throughout the cytoplasm in control cells (Fig. S2*A*) but were much less in APPwt (Fig. S2*B*) or APPswe M17 cells (Fig. S2*C*). Instead, mitochondria became significantly shorter and fatter, with a slight but significant increase in size in these cells (Fig. S2*E*). Total mitochondrial number was decreased while the number of damaged mitochondria in APPwt or APPswe M17 cells (Fig. S2*D*) was increased compared with control cells.

Effects of Aβ Production on Mitochondrial Dynamics. As there was no correlation between APP levels and severity of mitochondrial defects, we speculated that Aβ production was involved. Secreted $A\beta_{1-42}$ levels in the medium were measured and correlated with the percentage of cells exhibiting abnormal mitochondrial distribution or morphology in each of these lines (Fig. S3*A*). A significant positive correlation was found between Aβ levels and the percentage of cells with abnormal mitochondrial distribution ($r^2 = 0.938$, $P < 0.01$) and the percentage of cells with fragmented mitochondria ($r^2 = 0.958$, $P < 0.01$). Likewise, we found a significant negative correlation between Aβ levels and the percentage of cells with normal mitochondrial morphology ($r^2 = 0.946$, $P < 0.01$).

To corroborate the role of Aβ production, we transiently transfected control M17 cells with DsRed-tagged APPwt or APPswe constructs in the presence or absence of β-site APP-cleaving enzyme (BACE) inhibitor IV, which is able to efficiently prevent Aβ production without affecting APP expression. Mito-AcGFP was co-transfected to label mitochondria. Forty-eight hours after transfection, cells were fixed and immunostained with an antibody against tubulin to label the cell shape. Positively co-transfected cells were selected by the presence of both DsRed and AcGFP fluorescence signals (Fig. S3*B*). As previously reported, BACE inhibitor IV did not increase cell death in M17 cells (not shown), and it did not cause any mitochondrial abnormality (Fig. S3 *B–D*). Consistent with the observations in stable lines, transient overexpression of APPwt or APPswe also resulted in a significantly increased percentage of cells with fragmented mitochondria (Fig. S3*C*) and abnormal mitochondrial distribution (Fig. S3*D*). In both cases, BACE inhibitor IV, by blocking Aβ production (not shown), efficiently prevented mitochondrial abnormalities, suggesting that Aβ overproduction is responsible for these mitochondrial abnormalities.

Effects of APP Expression on Mitochondrial Fusion. Given the alterations in mitochondrial morphology, it is likely an impaired balance of fission/fusion is involved. To measure the occurrence of mitochondrial fusion events, stable M17 cell lines were transfected with a photo-convertible fluorescence protein, Mito-Dendra2, which can

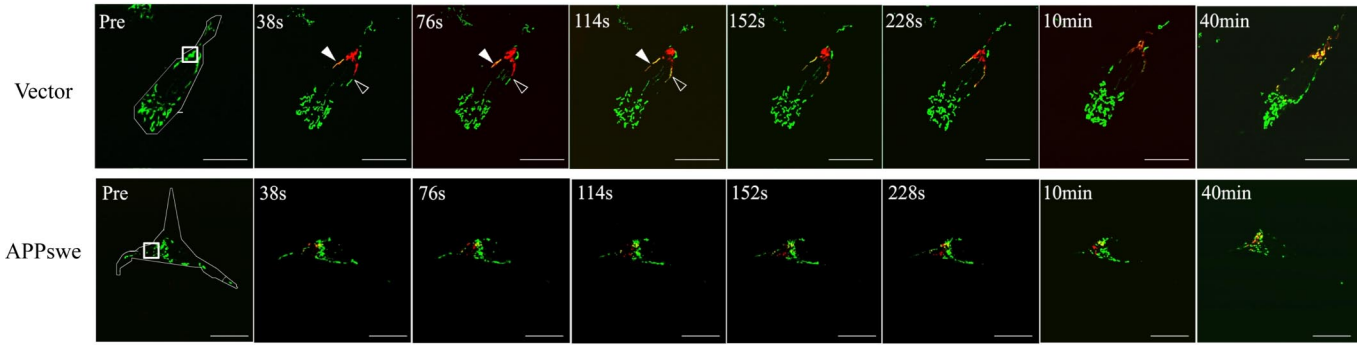

Fig. 2. APP expression affects mitochondrial fusion. M17 cells were transfected with mito-Dendra2 to label mitochondria. Before photo-conversion (Pre), Dendra2 emits green fluorescence. At time 0, laser activation is applied to ROI (square box) to allow full photo-conversion, from green to red, of all of the mitochondria within the ROI. Thereafter, mitochondrial behavior in the entire cell was monitored for 60 min. Active mitochondria fission (filled arrowhead) and fusion (open arrowhead) of individual mitochondrion could be observed in the representative control cell. (Scale bars, 20 μm.)

be irreversibly converted from a green to a red fluorescent state upon laser activation. Forty-eight hours after transfection, plates were placed under a confocal microscope, and using a lower power laser, we were able to detect positively transfected cells with green signal (Fig. 2). Several positively transfected cells with similar shape were chosen, and laser activation was applied to a defined region of interest (ROI) of the same size in these cells to allow full photo-conversion, from green to red, of all of the mitochondria within the ROI. Thereafter, mitochondrial behavior in the entire cell was monitored for the following 60 min (Fig. 2). The percentage of red mitochondria that became yellow (i.e., fusion between red and green mitochondria) over time was measured as an overall index for fusion events (Fig. 2). It took ≈10 min for all of the red mitochondria to become yellow in control cells, compared with more than 20 min in APPwt M17 cells with normal mitochondrial distribution (Fig. 2). It took even longer (i.e., 40 min) in both APPwt M17 cells with abnormal mitochondrial distribution and in APPswe M17 cells. These data suggested mitochondrial fusion occurred significantly slower in APPwt and APPswe M17 cells compared with control cells.

Effects of APP Expression on Mitochondrial Fission/Fusion Proteins. We next investigated effect of APP overexpression on mitochondrial fission (i.e., DLP1 and Fis1) and fusion proteins (i.e., OPA1, Mfn1, and Mfn2). Immunoblot analysis revealed that DLP1 and OPA1 were significantly reduced whereas Fis1 levels were significantly increased in APPwt and APPswe M17 cells compared with control cells (Fig. 3*A* and *B*). Conversely, there were no significant changes in Mfn1 and Mfn2 levels. Correlation analysis (Fig. S4 *A*–*C*) revealed that the levels of DLP1 or OPA1 were negatively correlated with Aβ levels whereas Fis1 levels were positively correlated with Aβ levels ($P < 0.01$). Moreover, the expression of DLP1 or OPA1 demonstrated a significantly negative correlation whereas the expression of Fis1 demonstrated a significant positive correlation with percentage of cells displaying abnormal mitochondrial distribution or morphology induced by APP overexpression. Supporting a causative role of increased Aβ production, changes in the levels of these proteins were abrogated when APPwt or APPswe M17 cells were treated with BACE inhibitor IV (Fig. S4*D*).

Effects of DLP1 and OPA1 on APP-Induced Abnormal Mitochondrial Dynamics. To test whether DLP1, OPA1, and/or Fis1 played a direct role in APP-induced mitochondrial abnormalities, we transiently transfected stable APPwt or APPswe M17 cells with Myc-tagged DLP1 or OPA1. Mito-DsRed2 was co-transfected to label mitochondria (Fig. S5*A*). DLP1 overexpression resulted in an increased percentage of cells with fragmented mitochondria in APPwt M17 cells, without much change in APPswe M17 cells, whereas OPA1 overexpression rescued morphological abnormalities in these cells by significantly decreasing the percentage of cells with fragmented mitochondria and restoring the percentage of cells with normal-length mitochondria (Fig. S5*B*). Most interestingly, the percentage of APPwt or APPswe M17 cells with abnormal mitochondrial distribution (i.e., peri-nuclear accumulation) decreased significantly with DLP1 overexpression but remained unchanged with OPA1 overexpression (Fig. S5*C*). Fis1 knockdown by miR RNAi technique in APPwt or APPswe M17 cells (Fig. S6*A*) had no effect on either mitochondrial morphology or distribution (Fig. S5 *B* and *C*).

In these experiments, we noticed an interesting phenomenon: DLP1 overexpression also caused prominent changes in cell shape in almost all of the positively transfected APPswe M17 cells, as evidenced by the appearance of longer processes even without RA treatment; these processes always contained mitochondria spanning the full length (Fig. S5*A*). We suspected that DLP1 overexpression in APPswe M17 cells may restore their ability to differentiate upon RA treatment. To test this hypothesis, we generated a stable M17 cell line overexpressing both APPswe and DLP1 (APPswe/DLP1 M17 cells). Immunoblot analysis confirmed the

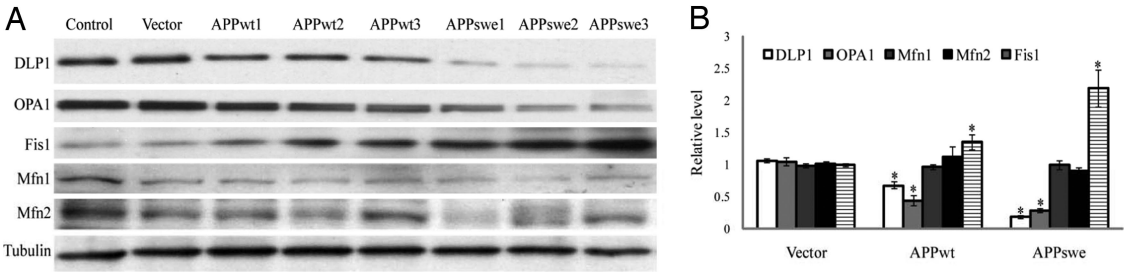

Fig. 3. APP expression modulates mitochondrial fission/fusion proteins. Representative immunoblot (*A*) and quantification analysis (*B*) revealed that DLP1 and OPA1 were reduced, whereas Fis1 was increased significantly in APPwt and APPswe M17 cells (*, $P < 0.05$).

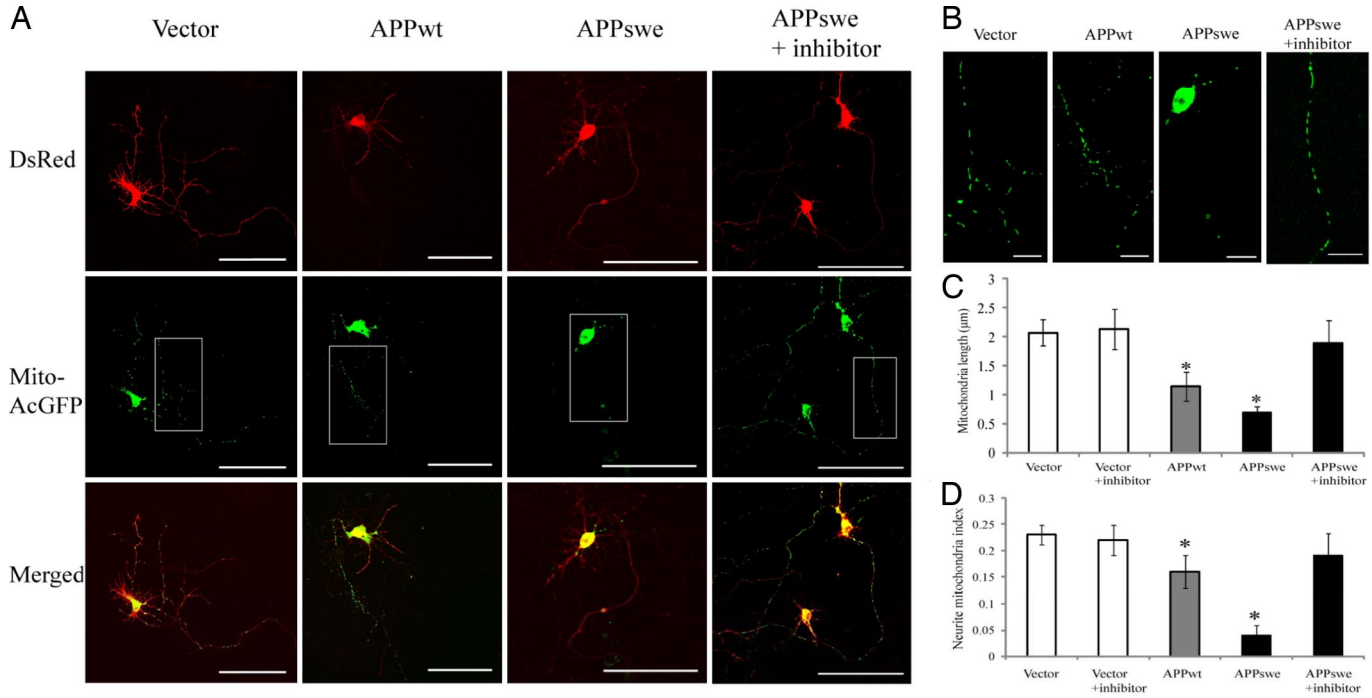

Fig. 4. APP causes abnormal mitochondrial dynamics in differentiated rat E18 primary hippocampal neurons. Neurons (DIV7) were co-transfected with mito-AcGFP and DsRed-tagged APP or APPswe in the absence or presence of 20 nM BACE inhibitor IV. Three days after transfection, neurons were fixed and evaluated. (*A*) Representative pictures of positively transfected neurons with different mitochondrial morphology and distribution pattern were shown. Red, DsRed-APP; green, mito-AcGFP. (Scale bar, 100 μm.) (*B*) Higher magnification pictures of the boxed area in *A*. (Scale bar, 20 μm.) (*C* and *D*) Mitochondria (length and coverage) in a segment of neuronal process at least 200 μm in length beginning from the cell body of neurons were analyzed. At least 20 cells were analyzed each time in three independent experiments.

restoration of DLP1 levels in APPswe/DLP1 M17 cells and the restoration of DLP1 expression did not affect APPswe expression (Fig. S6*B*). Indeed, at 1 month of RA treatment, ≈50% APPswe/DLP1 M17 cells extended long and branched neurites (Fig. S6*C*), similar to that of control M17 cells, suggesting that DLP1 overexpression restored the capability of differentiation in APPswe M17 cells. However, the stable M17 cell line overexpressing APPswe and OPA1 still failed to differentiate on RA treatment (Fig. S6*C*).

Effects of DLP1 and OPA1 on APP-Induced Mitochondrial Functional Changes. Because mitochondrial morphology is critical for function, we investigated the effect of APP overexpression on mitochondrial function and the effect of DLP1 or OPA1 expression. Mitochondria are the primary source for endogenous ROS. ROS levels were significantly enhanced in APPwt M17 cells and even more so in APPswe M17 cells (Fig. S7*A*). Although transient overexpression of DLP1 or OPA1 did not change the basal ROS levels in normal M17 cells, conversely, transient overexpression of DLP1 resulted in a further increase of ROS levels in APPwt M17 cells, but not much change in APPswe M17 cells, and transient overexpression of OPA1 in either APPwt or APPswe M17 cells resulted in a significant decrease in ROS levels comparable to control level. We also measured mitochondrial membrane potential (MMP) using the fluorescence dye Rodamine 123 (Fig. S7*B*). To control for the difference in mitochondria numbers in different lines, we also measured the fluorescence intensity of MMP-independent dye Mitotracker Red 580 FM. The relative MMP (i.e., ratio of intensity with Rodamine 123 to Mitotracker Red 580 FM) was significantly decreased in APPwt and APPswe M17 cells. Transient overexpression of DLP1 caused decreased MMP whereas transient overexpression of OPA1 caused increased MMP in normal M17 cells. Importantly, transient overexpression of DLP1 in APPwt or APPswe M17 cells caused a further significant decrease in MMP whereas overexpression of OPA1 partially rescued the decrease of MMP in these two lines. ATP production was significantly decreased in APPwt and APPswe M17 cells (Fig. S7*C*). Transient overexpression of DLP1 had no effect, whereas transient overexpression of OPA1 caused increased ATP production in normal M17 cells. Similarly, transient DLP1 overexpression had no effect, whereas transient overexpression of OPA1 partially restored ATP production in APPwt and APPswe M17 cells.

Effects of APP Expression and Aβ-Derived Diffusible Ligands on Mitochondrial Dynamics in Primary Neurons. To determine whether APP expression has similar effects in differentiated neuronal cells, rat E18 primary hippocampal neurons (7 days *in vitro* [DIV]) were transiently co-transfected with mito-AcGFP and DsRed-tagged APP. Seventy-two hours after transfection, positively co-transfected cells with the presence of both DsRed and AcGFP fluorescence signals were analyzed (Fig. 4). Mitochondrial length in neuronal processes was decreased significantly in control cells (2.1 ± 0.24 μm) compared with APPwt- overexpressing cells (1.1 ± 0.25 μm) and APPswe-overexpressing cells (0.7 ± 0.11 μm). Mitochondrial density in neuronal processes also decreased significantly in control neurons (0.11 ± 0.012 μm) and APPwt-overexpressing neurons (0.14 ± 0.031 μm) compared with APPswe-overexpressing neurons (0.04 ± 0.017 μm). The overall mitochondrial coverage in neuronal processes, as indicated by neurite mitochondria index (i.e., total mitochondrial length/neurite length) (21), was significantly decreased in neurons overexpressing APPwt (0.16 ± 0.031) or APPswe (0.04 ± 0.019) compared with control neurons (0.22 ± 0.013). Moreover, APP-induced mitochondrial changes were completely prevented by BACE inhibitor IV treatment (Fig. 4), suggesting that these effects were mediated by Aβ production.

To directly test the effect of Aβ on mitochondrial dynamics, we treated primary hippocampal neurons (DIV = 7) with 800-nM Aβ-derived diffusible ligands (ADDLs), a condition that did not cause significant cell death, and found that ADDLs led to a

significant decrease in mitochondrial length, mitochondrial density, and overall mitochondrial coverage in neuronal processes (data not shown). As a control, $A\beta_{42-1}$ (10 μM) had no effect on any of these parameters.

Discussion

In this study, we show that APP overexpression, likely through increased production of Aβ, results in perturbed mitochondrial dynamics, which impact mitochondrial function and neuronal function. Specifically, we found that APP overexpression induced mitochondrial fragmentation and abnormal mitochondrial distribution in M17 cells and rat primary hippocampal neurons. That these effects were completely prevented by BACE inhibitor IV treatment and that ADDL treatment also led to similar mitochondrial changes suggest that Aβ production mediated APP-induced mitochondrial abnormalities. Although perturbation in cellular metabolism, energy status, and redox homeostasis may affect mitochondrial dynamics (22), it is likely that APP affects mitochondrial dynamics directly through the differential modulation of mitochondrial fission and fusion proteins that cause an impaired balance of mitochondrial fission/fusion, rather than indirectly through perturbation of mitochondrial function, because manipulations of DLP1 or OPA1 rescued the effect of APP overexpression, resulting in a restored cellular capability to differentiate upon RA treatment and mitochondrial functions such as MMP and ATP production and lowered ROS levels.

One major observation of this study is that APP overexpression causes mitochondrial fragmentation in neurons, as evidenced by both confocal and electron microscopy. Because mitochondrial morphology is tightly controlled by the balance of mitochondrial fission and fusion (16), we hypothesized that APP-induced mitochondrial fragmentation was caused by enhanced fission, reduced fusion, or both. In support of this notion, using photo-convertible fluorescence labeling, we were able to demonstrate that mitochondria in APP-overexpressing cells are able to fuse, but at a significantly slower rate than control cells. It is unclear whether an increased fission rate is also involved in our models. In line with the suggestion of an impaired balance of mitochondrial fission and fusion, we found that APP overexpression reduced the levels of DLP1 and OPA1 and increased the levels of Fis1. Although decreased expression of DLP1 or Fis1 can lead to mitochondrial elongation while decreased expression of OPA1 or increased expression of Fis1 is more typically thought to effect fragmentation (18, 23–25), recent studies show that decreased expression of both Fis1 and OPA1 actually led to mitochondrial fragmentation (26, 27). We also found that mitochondria become fragmented when both DLP1 and OPA1 were decreased (data not shown), indicating that mitochondria are predominantly fragmented when both fission and fusion proteins are perturbed. This is consistent with our observation of mitochondrial fragmentation in APP-overexpressing M17 cells in which DLP1, OPA1, and Fis1 are all perturbed. Indeed, it was the manipulation of OPA1 but not DLP1 or Fis1 that rescued APP-induced mitochondrial fragmentation. It is known that changes in mitochondrial morphology may affect mitochondrial function (18, 19). In this regard, it is important to note that mitochondrial dysfunction, including increased ROS levels and reduced MMP and ATP production, were observed in APPwt and APPswe M17 cells in which mitochondrial fragmentation was also observed. Therefore, it is likely that enhanced mitochondrial fragmentation contributes to APP-induced mitochondrial dysfunction. In support of this, overexpression of OPA1 in APPwt or APPswe M17 cells partially rescued mitochondrial fragmentation, restored normal mitochondrial morphology, and also partially rescued mitochondrial functional parameters. Conversely, overexpression of DLP1 had little effect or even exacerbated mitochondrial fragmentation and failed to rescue mitochondrial functional parameters. Nevertheless, given the presence of APP in mitochondria (Fig. S8) and its interaction with mitochondrial proteins, the possibility that APP may also induce mitochondrial dysfunction through other pathways cannot be ruled out.

Another notable aspect of the perturbed mitochondrial dynamics induced by APP overexpression observed in neurons is the abnormal mitochondrial distribution (i.e., perinuclear accumulation). Mitochondrial fission and fusion proteins regulate mitochondrial distribution (25, 28), and we found reduced DLP1 and OPA1 and increased Fis1 in cells overexpressing APP. It is of interest to note that reduced DLP1 or OPA1 expression or increased Fis1 expression alone, despite their differential effects on mitochondrial morphology, all cause perinuclear accumulation of mitochondria in non-neuronal cells (25, 28, 29). However, suggestive of a dominant pathway, it is likely that DLP1 plays a major role in APP-induced abnormal mitochondrial distribution as the overexpression of DLP1, but not manipulations of OPA1 or Fis1, rescued perinuclear mitochondrial accumulation. Indeed, we recently reported a similar abnormal mitochondrial distribution as a prominent feature in AD fibroblasts that could also be rescued by overexpression of DLP1 (20). Because DLP1 failed to rescue APP-induced mitochondrial dysfunction (i.e., ROS, MMP, and ATP), it appears that the abnormal mitochondrial distribution had minimal impact on mitochondrial function parameters measured in this study; however, more subtle changes may not be ruled out. In this regard, it is notable that APPswe M17 cells exhibit a profound cellular dysfunction such that they lose the capability to differentiate upon RA induction, which is consistent with a previous report in N2a cells (30). Interestingly, we found that DLP1 overexpression rescued this differentiation deficiency in APPswe M17 cells. The rescue effect of DLP1 overexpression is most likely a result of the restoration of mitochondrial distribution rather than influence on mitochondrial morphology/function because (*i*) DLP1 overexpression failed to rescue mitochondrial fragmentation and functions and (*ii*) conversely, overexpression of OPA1, which rescued mitochondrial morphology/functions but not abnormal mitochondrial distribution, failed to rescue the differentiation deficiency. There are several implications of this observation. First, it is likely critical for mitochondria to be distributed evenly during differentiation, implicating a local support closer to plasma membrane from mitochondria is essential, which is likely lost in APPswe M17 cells. Second and more importantly, abnormal mitochondrial distribution must have caused some cellular functional deficits that eventually manifest as differentiation deficiency upon RA induction. Although the nature of such deficits are still unclear, it likely involves deficiency of local mitochondrial support, which can be very subtle and become apparent only in high-demand situations and may be exacerbated in very polarized cells such as differentiated neurons. In this regard, we also found that APP overexpression or ADDL treatment caused mitochondrial fragmentation and reduced mitochondrial coverage in neuronal processes in differentiated primary hippocampal neurons. Indeed, synaptic terminals have abundant mitochondria essential to meet the local demand (31), and the paucity of mitochondria leads to synaptic dysfunction in both dendrites and axons (21, 32). Not coincidentally, synaptic abnormalities were reported in APPswe neurons and transgenic mice (33). Therefore, it is likely that APP overexpression, by down-regulating DLP1 and causing abnormal mitochondrial distribution, depletes local mitochondrial support at remote sites and causes synaptic dysfunction. Indeed, our preliminary studies suggest that DLP1 levels are also reduced in Tg2576 APP transgenic mice (data not shown), and we are investigating whether APP-induced DLP1 reduction also leads to abnormal mitochondrial distribution and synaptic dysfunction in transgenic models.

Taken together, the findings presented here suggest that abnormal mitochondrial dynamics are likely involved in mitochondrial and neuronal dysfunction in the brain of patients with AD with APP mutations. However, as similar abnormalities in mitochondria are also evident features of fibroblasts from sporadic AD cases (20), it is likely that abnormal mitochondrial dynamics may be a feature of

all AD cases, sporadic or familial. Such a notion is consistent with the decreased number but increased size of mitochondria in vulnerable neurons in the biopsied AD brain (9). In re-analyzing this same data set (9), we found that AD neurons exhibited significantly reduced length (Fig. S9) with a significant increase in overall size (9). These *in vivo* findings are very similar to what is reported here in APPwt and APPswe M17 cells. Overall, such data indicate a balance tipped toward more mitochondrial fission may be in play in AD neurons, and modulation of mitochondrial dynamics may prove to be a valuable therapeutic target of AD. Given the critical role of mitochondria in neurons, especially at the tips of axon or dendrite, it is very likely that abnormal mitochondrial dynamics may be a common pathway leading to cellular dysfunction critical to various neurodegenerative diseases. In this regard, it is worth noting that PINK1, mutations of which lead to Parkinson disease, appears to play a role in mitochondrial fission through regulation of DLP1 (34), and fibroblasts from patients with Parkinson disease bearing PINK1 mutations also exhibit abnormal mitochondrial morphology (35).

Materials and Methods

Cell Culture and Transfection. Human neuroblastoma M17 cells were grown as described before (36). Transfection was performed using Effectene (Qiagen) (20) and 300 μg/ml geneticin (Invitrogen) or 400 μg/ml of hygromycin B (Calbiochem) was included in the medium for stable cell line selection. Stable cell lines were maintained with 100 μg/ml geneticin or 200 μg/ml of hygromycin.

Expression Vectors, Antibodies, Cell Treatments and Measurements, Western Blot Analysis, Electron Microscopy, Immunofluoresence, and Time Lapse Imaging. See *SI Materials and Methods*.

Quantification of Mitochondrial Distribution. For each cell line, at least 1,000 cells were measured. Staining for tubulin allowed for visualization and measurement of the total cellular area (i.e., total cytoplasmic area). Mitochondria were labeled by Mito-DsRed. A boundary line was drawn along bordering mitochondria to encircle an area containing all mitochondria within the cell, the size of the cytoplasmic area outside this circled area was measured (i.e., cytoplasmic area devoid of mitochondria), and its ratio to total cytoplasmic area was calculated and presented as a percentage. Comparing to control cells, the percentage of the cytoplasmic area devoid of mitochondria was approximately fourfold larger in APPwt M17 cells and $\approx$15-fold larger in APPswe M17 cells. Based on the fact that more than 95% of control cells exhibited less than 10% cytoplasmic areas devoid of mitochondria (Fig. S1), we defined those cells containing more than 10% cytoplasmic areas devoid of mitochondria as cells with abnormal mitochondria distribution.

ACKNOWLEDGMENTS. This work was funded by National Institutes of Health grant AG031852 and Alzheimer's Association grant IIRG-07–60196. We thank Drs. Yisang Yoon (University of Rochester, Rochester, NY) Huaxi Xu (The Burnham Institute, La Jolla, CA) and Luca Scorrano (Venetian Institute of Molecular Medicine, Venice, Italy) for providing reagents, and George Perry and Mark A. Smith (Case Western Reserve University) for providing electron micrographs.

1. Zheng H, Koo EH (2006) The amyloid precursor protein: beyond amyloid. *Mol Neurodegener* 1:5.
2. Hardy J, Selkoe DJ (2002) The amyloid hypothesis of Alzheimer's disease: progress and problems on the road to therapeutics. *Science* 297:353–356.
3. Nunomura A, *et al.* (2006) Involvement of oxidative stress in Alzheimer disease. *J Neuropathol Exp Neurol* 65:631–641.
4. Bogdanovic N, Zilmer M, Zilmer K, Rehema A, Karelson E (2001) The Swedish APP670/671 Alzheimer's disease mutation: the first evidence for strikingly increased oxidative injury in the temporal inferior cortex. *Dementia Geriatr Cogn Disord* 12:364–370.
5. Pratico D, Uryu K, Leight S, Trojanoswki JQ, Lee VM (2001) Increased lipid peroxidation precedes amyloid plaque formation in an animal model of Alzheimer amyloidosis. *J Neurosci* 21:4183–4187.
6. Zhu X, Smith MA, Perry G, Aliev G (2004) Mitochondrial failures in Alzheimer's disease. *Am J Alzheimers Dis Other Demen* 19:345–352.
7. Wallace DC (1999) Mitochondrial diseases in man and mouse. *Science* 283:1482–1488.
8. Coskun PE, Beal MF, Wallace DC (2004) Alzheimer's brains harbor somatic mtDNA control-region mutations that suppress mitochondrial transcription and replication. *Proc Natl Acad Sci USA* 101:10726–10731.
9. Hirai K, *et al.* (2001) Mitochondrial abnormalities in Alzheimer's disease. *J Neurosci* 21:3017–3023.
10. Baloyannis SJ (2006) Mitochondrial alterations in Alzheimer's disease. *J Alzheimers Dis* 9:119–126.
11. Lustbader JW, *et al.* (2004) ABAD directly links Abeta to mitochondrial toxicity in Alzheimer's disease. *Science* 304:448–452.
12. Devi L, Prabhu BM, Galati DF, Avadhani NG, Anandatheerthavarada HK (2006) Accumulation of amyloid precursor protein in the mitochondrial import channels of human Alzheimer's disease brain is associated with mitochondrial dysfunction. *J Neurosci* 26:9057–9068.
13. Manczak M, *et al.* (2006) Mitochondria are a direct site of A beta accumulation in Alzheimer's disease neurons: implications for free radical generation and oxidative damage in disease progression. *Human Mol Genet* 15:1437–1449.
14. Reddy PH, *et al.* (2004) Gene expression profiles of transcripts in amyloid precursor protein transgenic mice: up-regulation of mitochondrial metabolism and apoptotic genes is an early cellular change in Alzheimer's disease. *Hum Mol Genet* 13:1225–1240.
15. Rui Y, Tiwari P, Xie Z, Zheng JQ (2006) Acute impairment of mitochondrial trafficking by beta-amyloid peptides in hippocampal neurons. *J Neurosci* 26:10480–10487.
16. Chan DC (2006) Mitochondria: dynamic organelles in disease, aging, and development. *Cell* 125:1241–1252.
17. Okamoto K, Shaw JM (2005) Mitochondrial morphology and dynamics in yeast and multicellular eukaryotes. *Ann Rev Genet* 39:503–536.
18. Chen H, Chomyn A, Chan DC (2005) Disruption of fusion results in mitochondrial heterogeneity and dysfunction. *J Biol Chem* 280:26185–26192.
19. Chen H, *et al.* (2003) Mitofusins Mfn1 and Mfn2 coordinately regulate mitochondrial fusion and are essential for embryonic development. *J Cell Biol* 160:189–200.
20. Wang X, Su B, Fujioka H, Zhu X (2008) Dynamin-like protein 1 reduction underlies mitochondrial morphology and distribution abnormalities in fibroblasts from sporadic Alzheimer's disease patients. *Am J Pathol* 173:470–482.
21. Li Z, Okamoto K, Hayashi Y, Sheng M (2004) The importance of dendritic mitochondria in the morphogenesis and plasticity of spines and synapses. *Cell* 119:873–887.
22. Ichishita R, *et al.* (2008) An RNAi screen for mitochondrial proteins required to maintain the morphology of the organelle in Caenorhabditis elegans. *J Biochem* 143:449–454.
23. Smirnova E, Griparic L, Shurland DL, van der Bliek AM (2001) Dynamin-related protein Drp1 is required for mitochondrial division in mammalian cells. *Mol Biol Cell* 12:2245–2256.
24. Griparic L, van der Wel NN, Orozco IJ, Peters PJ, van der Bliek AM (2004) Loss of the intermembrane space protein Mgm1/OPA1 induces swelling and localized constrictions along the lengths of mitochondria. *J Biol Chem* 279:18792–18798.
25. Frieden M, *et al.* (2004) Ca(2+) homeostasis during mitochondrial fragmentation and perinuclear clustering induced by hFis1. *J Biol Chem* 279:22704–22714.
26. Lee S, *et al.* (2007) Mitochondrial fission and fusion mediators, hFis1 and OPA1, modulate cellular senescence. *J Biol Chem* 282:22977–22983.
27. Lee YJ, Jeong SY, Karbowski M, Smith CL, Youle RJ (2004) Roles of the mammalian mitochondrial fission and fusion mediators Fis1, Drp1, and Opa1 in apoptosis. *Mol Biol Cell* 15:5001–5011.
28. Smirnova E, Shurland DL, Ryazantsev SN, van der Bliek AM (1998) A human dynamin-related protein controls the distribution of mitochondria. *J Cell Biol* 143:351–358.
29. Misaka T, Miyashita T, Kubo Y (2002) Primary structure of a dynamin-related mouse mitochondrial GTPase and its distribution in brain, subcellular localization, and effect on mitochondrial morphology. *J Biol Chem* 277:15834–15842.
30. Wang YP, Wang ZF, Zhang YC, Tian Q, Wang JZ (2004) Effect of amyloid peptides on serum withdrawal-induced cell differentiation and cell viability. *Cell Res* 14:467–472.
31. Ly CV, Verstreken P (2006) Mitochondria at the synapse. *Neuroscientist* 12:291–299.
32. Verstreken P, *et al.* (2005) Synaptic mitochondria are critical for mobilization of reserve pool vesicles at Drosophila neuromuscular junctions. *Neuron* 47:365–378.
33. Almeida CG, *et al.* (2005) Beta-amyloid accumulation in APP mutant neurons reduces PSD-95 and GluR1 in synapses. *Neurobiol Dis* 20:187–198.
34. Poole AC, *et al.* (2008) The PINK1/Parkin pathway regulates mitochondrial morphology. *Proc Natl Acad Sci USA* 105:1638–1643.
35. Exner N, *et al.* (2007) Loss-of-function of human PINK1 results in mitochondrial pathology and can be rescued by parkin. *J Neurosci* 27:12413–12418.
36. Zhu X, *et al.* (2004) Neuroprotective properties of Bcl-w in Alzheimer disease. *J Neurochem* 89:1233–1240.